Downloaded from orbit.dtu.dk on: May 05, 2023

DTU Library

Active control: Wind turbine model

Bindner, H.

Publication date:
1999

Document Version
Publisher's PDF, also known as Version of record

Link back to DTU Orbit

Citation (APA):
Bindner, H. (1999). *Active control: Wind turbine model*. Denmark. Forskningscenter Risoe. Risoe-R No. 920(EN)

General rights
Copyright and moral rights for the publications made accessible in the public portal are retained by the authors and/or other copyright owners and it is a condition of accessing publications that users recognise and abide by the legal requirements associated with these rights.

- Users may download and print one copy of any publication from the public portal for the purpose of private study or research.
- You may not further distribute the material or use it for any profit-making activity or commercial gain
- You may freely distribute the URL identifying the publication in the public portal

If you believe that this document breaches copyright please contact us providing details, and we will remove access to the work immediately and investigate your claim.

Risø-R-920(EN)

Active Control: Wind Turbine Model

Henrik Bindner

Risø National Laboratory, Roskilde, Denmark
July 1999

Abstract

Denne rapport er en del af rapporteringen af arbejdet udført i projektet 'Aktiv regulering og vindmølledynamik'. Projektet er støttet af Energistyrelsen under EFP91, ENS j.nr. 1364/91-0003. Projektdeltagere er Vestas Wind Systems A/S, Kurt Andersen DTU og Forskningscenter Risø.

Projektet har til formål at undersøge anvendelse af aktiv regulering og analysere vekselvirkninger med vindmøllens dynamik med henblik på optimering af energiproduktion, forbedring af effektbegrænsning og minimering af de strukturelle laster. Målinger og eksperimenter er udført på en Vestas WD34 400kW pitchreguleret vindmølle.

Denne rapport omhandler optimering af regulatorerne, primært til forbedring af effektbegrænsning. Regulatoroptimeringen er opdelt i tre faser. I den første fase undersøges den eksisterende PID-regulering af effekten på WD34 gennem målinger. I anden fase opbygges en reguleringsteknisk model af en vindmølle med variabel bladvinkel. Den benyttes til optimering af PID-regulatoren. Undersøgelsernes resultater prøves på WD34. I tredje fase undersøges mere avancerede reguleringsmetoder.

Både målinger og simuleringer har vist at det ikke er muligt at opnå store forbedringer at reguleringskvaliteten ved anvendelse af PID-regulatorer. Det er nødvendigt at have en meget differentierende regulator. En sådan regulator gør systemet mere følsomt overfor bla. støj og parameterændringer. Anvendelsen af LQG-regulatorer kunne have forbedret reguleringskvaliteten, idet LQG-regulatorer er modelbaserede og derfor indeholder en større viden om det system, der skal reguleres. Imidlertid gælder der den samme begrænsning, at regulatoren for at opnå en tilstrækkelig båndbredde bliver meget følsom over for støj og modelunøjagtigheder. Resultaterne fra testene med LQG-regulatorer har vist, at det er meget vigtigt at inkludere robustheds-betragtninger i designet af mere avancerede regulatorer.

De opbyggede modeller kan anvendes til design af regulatorer til variabelt omløbstal vindmøller med tilføjelsen af en frekvensomformer model.

2216-25

ISBN 87-550-~~2381-9~~
ISSN 0106-2840
Afdelingen for Informationservice - Risø- 1999

DISCLAIMER

Portions of this document may be illegible in electronic image products. Images are produced from the best available original document.

Contents

1 Introduction

This report presents a model for design and analysis of controllers for pitch controlled wind turbines in order to evaluate and improve pitch controllers for conventional three bladed pitch controlled wind turbines.

The work presented is supported by the Danish Energy Agency with the participation of Vestas Wind Systems and The Technical University of Denmark. The title of the project is 'Active control and wind turbine dynamics'.

The main objective of the project is to establish a validated foundation for design and analysis of controllers for pitch control and to study different control strategies through both simulation and measurements.

The work was initiated in order to improve the understanding of the relationship between the wind turbine, especially the structural and aerodynamic part, and the control strategy as well as selected controller parameters.

The other important project objective is the evaluation of different controllers tested on the wind turbine.

In Denmark there has been three activities related to pitch controllers. The first activity is Vestas together with Kurt Andersen. This work has not been published. The modelling work in this report is based on the models used by Vestas. The second is the work done in connection to the Nibe B turbine and the Tjæreborg turbine. These are large utility developed turbines both employing pitch control for power limitation. Typically this work has not been in a form usually used for design of controllers, (eg. Madsen & Frandsen, 1989). The third activity centered around Denmarks Technical University. The work done there has concentrated on the use of sophisticated control algorithms and strategies. The models have not been validated and the designed controllers have not been tested on a real turbine, (Knudsen, 1983, Klingenberg, 1991, Jørgensen, 1993, Ma Xin, 1993).

Internationally there has been done several studies on pitch control. The main contributers are in UK, The Netherlands and in Sweden. In UK Wind Energy Group and University of Strathclyde have worked with adaptive control (WEG, 1989, Bossanyi, 1989) and both classical and robust control using simple models (Wilkie et al, 1990, Grimble et al, 1990, Leithead et al, 1990). In the Netherlands Delft University of Technology has developed the non-linear simulation code DUWECS and has used it for design of advanced controllers (Bongers et al, 1989, Bongers et al, 1993, Bongers et al, 1993b). These controllers include optimal control and $H\infty$ control. In Sweden there has also been some studies eg. (Mattson 1993).

The modelling work in the report is based on physical models suitable for controller design and analysis, that is first order linear differential equations. Various model complexities are studied and the model selection is based on measurements on a Vestas Wind Systems WD34 400 kW full span pitch controlled three bladed wind turbine.

The wind turbine model that is presented in this report includes tower and blade bending, gearbox, generator, pitch system, aerodynamics and the controller. The model is verified by measurements.

The model enables the design of pitch controllers and allows for comparison of different designs. The report also gives guidelines for optimization of various model parameters in order to improve the controllers performance.

2 Description of the model

In this chapter a wind turbine model is presented. The purpose of the model is to predict the behavior the wind turbine sufficiently well for design and analysis of controllers for power limitation. In this respect it is important that the model is simple and linear. Also the model has to be detailed enough to be used to optimize the controllers.

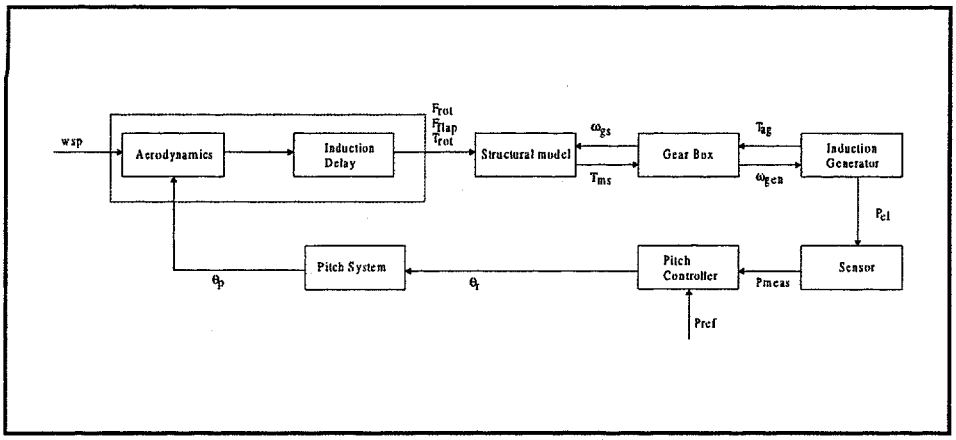

figure 1 Model overview (submodels and main variables)

The wind turbine model is built from several submodels or component models. These models describe the combined interaction by the wind and pitch angle with the aerodynamics of the rotor to produce the torque on the main shaft and the forces on the tower and blade (flapwise). The torque is converted to electrical power through the gear box and the induction generator. Measured power is fed back through the pitch controller to the pitch system that changes the actual pitch angle. These models are interconnected to form the total model, figure 1.

Each of the different submodels are described below.

The models are implemented in MATLAB/SIMULINK, (Matlab 94).

2.1 Structural Model: Tower, blade and main shaft

To describe the impact of the dynamical behaviour of the wind turbine a simple model is formulated. The model includes the first tower bending mode, the symmetrical flap bending mode and the torsion of the main shaft, figure 1. The derivation of the equations is in Appendix A.

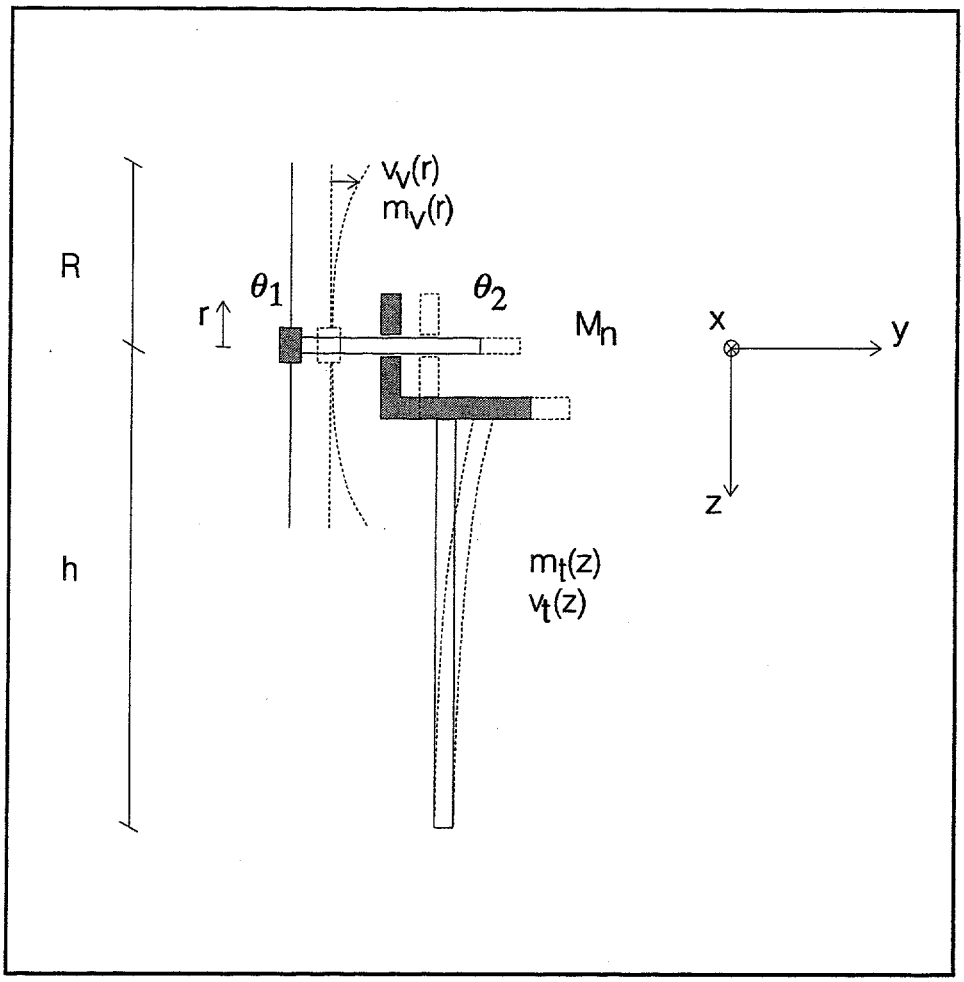

figure 2 Tower and Rotor bending

The equations have the form

$$M\ddot{x} + C\dot{x} + Kx = Q \tag{1}$$

where $\boldsymbol{M}$ is the mass matrix

$$M = \begin{bmatrix} M_n + \tilde{m}_t + 3\tilde{m}_v^1 & 3\tilde{m}_v^2 & 0 & 0 \\ 3\tilde{m}_v^2 & 3\tilde{m}_v^3 & 0 & 0 \\ 0 & 0 & 3\tilde{m}_v^4 & 0 \\ 0 & 0 & 0 & 0 \end{bmatrix} \tag{2}$$

and $\boldsymbol{K}$ is the stiffness matrix

$$K=\begin{bmatrix} K_t & 0 & 0 & 0 \\ 0 & 3K_v & 0 & 0 \\ 0 & 0 & K_{ms} & -K_{ms} \\ 0 & 0 & -K_{ms} & K_{ms} \end{bmatrix} \tag{3}$$

And $\boldsymbol{C}$ is the damping which is assumed to proportional to the stiffness

$$C=diag(c_1,c_2,c_3,c_4)*K \tag{4}$$

The state vector, $\boldsymbol{x}$, is

$$x=\begin{bmatrix} u_t & u_b & \theta_{rs} & \theta_{gs} \end{bmatrix}^T \tag{5}$$

where

$\boldsymbol{u_t}$	nacelle position
$\boldsymbol{u_b}$	tip position
$\boldsymbol{\theta_{rs}}$	angular position of main shaft at rotor end
$\boldsymbol{\theta_{gs}}$	angular position of main shaft at gear box end

The matrix $\boldsymbol{Q}$ is the load on the system. The load consists of the thrust on the whole rotor, thrust on the blades and torque on the main shaft. These loads are highly non-linear and depend on the wind speed and pitch angle as well as on the velocity of the nacelle tip and rotor (and the rotor speed). To make the model operational the loads are linearized at an operation point. Disregarding higher than first-order terms of the state vector, this splits $\boldsymbol{Q}$ in three parts.

$$Q=Q_1\begin{bmatrix} \Delta u_w \\ \Delta\theta_p \end{bmatrix}+Q_2\dot{x}+Q_0 \tag{6}$$

The first part is the dynamic load and depends on the wind speed and pitch angle (deviations from operation point), Q_2 is the aerodynamic damping. Q_0 is the mean load at the operation point. The aerodynamic damping can be both positive and negative depending on the operation point.

How the different elements of the matrices are found is also described in appendix A.

The equations are reformulated in state space form with the loads and the angular velocity of the main shaft at the gear box end as inputs and with the main shaft torque as output. Details are found in appendix A.

2.2 Gear box and generator rotor

The gear box and generator rotor inertia is modelled as two inertias with one spring and one damper between them, figure 3.

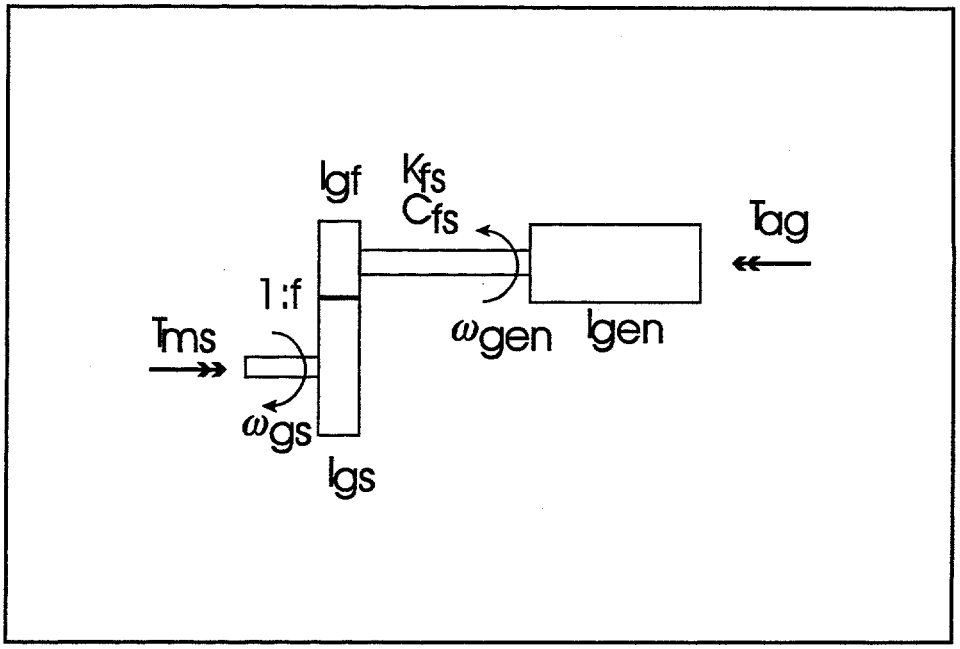

figure 3 Gear box and generator inertia model

The symbols in the figure are

I_{gs}, I_{gf}	inertia of gear on slow resp. fast side of the gear
I_{gen}	inertia of the generator rotor
f	gear ratio
K_{fs}	stiffness of the fast shaft
C_{fs}	damping of the fast shaft
T_{ms}	torque of the main shaft, input
T_{ag}	air gap (reaction) torque of the generator, input
ω_{gs}	angular velocity of the slow shaft on the gear box, output
ω_{gen}	angular velocity of generator rotor, output

The inputs to the model are the torque of the main shaft and the air gap torque of the generator. The outputs are the angular velocities of the main shaft in the gear box end and the generator rotor.

In the case of the WD34 the main contributors to the inertia, I_{gf}, and stiffness, K_{fs}, are the inertia of the brake and stiffness of the clutch placed on the fast shaft.

The equations describing the system

$$\begin{bmatrix} I_{gs}+f^2 I_{gf} & 0 \\ 0 & I_{gen} \end{bmatrix} \begin{bmatrix} \dot{\omega}_{gs} \\ \dot{\omega}_{gen} \end{bmatrix} + \begin{bmatrix} f^2 C_{fs} & -fC_{fs} \\ -fC_{fs} & C_{fs} \end{bmatrix} \begin{bmatrix} \omega_{gs} \\ \omega_{gen} \end{bmatrix} + \begin{bmatrix} fK_{fs} \\ -K_{fs} \end{bmatrix} (f\theta_{gs} - \theta_{gen}) = \begin{bmatrix} T_{ms} \\ T_{ag} \end{bmatrix} \quad (7)$$

The model is linear and has one eigenfrequency. The reason for this formulation is that there are only three independent states, the two angular velocities and the difference in angle of the inertias. This formulation, where the absolute angles are eliminated, is numerically better.

2.3 Induction Generator Model

The induction generator is modelled at three levels. The most detailed includes the dynamics of the stator and the rotor. The medium complex model includes only the rotor dynamics. The simple model is the static relation between torque and rpm of the rotor. The first two models are non-linear. The more complex models can be used to assess the mutual influence of the wind turbine and the grid on each other. The complex models can also be used when variable speed turbines are considered.

2.3.1 Model Description

The basis of the three models is a two-axis model of the generator, (Kovacs, 1984). The model is also used in (Bindner 1999) for assessing the drive train dynamics. The model is referred to as a d-q axis model. The generator is modelled with two perpendicular coils in both the stator and the rotor. The fluxes and voltages can then be represented by complex numbers. Saturation effects are not modelled. The generator is assumed to be in the same state of saturation. Only symmetrical loads are considered. The generator is assumed to be connected directly to a strong grid.

The basic dynamic and algebraic equations of the generator descibing the fluxes and the developed torque and power are (complex notation is used)

$$\frac{d\psi_s}{dt} = -(j\omega + \frac{R_s}{\sigma L_s})\psi_s + \frac{R_s L_M}{\sigma L_s L_r}\psi_r - u_s \tag{8}$$

$$\frac{d\psi_r}{dt} = -(j(\omega - \omega_r) + \frac{R_r}{\sigma L_r})\psi_r + \frac{R_r L_M}{\sigma L_s L_r}\psi_s \tag{9}$$

$$p_{el} = \frac{3}{2} Re(u_s^* (\frac{1}{\sigma L_s}\psi_s - \frac{L_M}{\sigma L_s L_r}\psi_r)) \tag{10}$$

$$T_{ag} = \frac{3}{2} Im(-\psi_s^* (\frac{1}{\sigma L_s}\psi_s - \frac{L_M}{\sigma L_s L_r}\psi_r)) \tag{11}$$

where

$$\sigma = 1 - \frac{L_M^2}{L_s L_r}$$

The symbols in the equations are

u_s	stator voltage
ψ_s	stator flux
ψ_r	rotor flux
ω	grid frequency
ω_r	generator rotor speed
p_{el}	electrical power
T_{ag}	reaction torque (airgap)

R_s	stator resistance
R_r	rotor resistance
L_s	stator inductance
L_r	rotor inductance
L_M	mutual inductance
σ	leakage factor

The first two equations describe the fluxes in the stator and rotor windings in the two directions. The next two describe the electrical power and the reaction torque.

The levels of complexity of modelling is related to whether the fluxes are allowed to change discontinuously or not. The detailed model consists of the equations (8) to (11). In the medium detailed model the flux in the stator is allowed to change discontinuously, that is the derivative is 0 (it is always in steady state). In the simple model the same is true for the rotor flux and the model is the same as the steady state model and the torque depends only on the slip.

The inputs to the model are the grid voltage and frequency, which are kept constant, and the rotor speed. The outputs are the airgap torque and the power.

In this context a linearised version of the medium complex model is used. Even though the dynamics are fast compared to the rest of the model the two states are kept in the model. This physical description of the generator makes it possible to study the current during a simulation together with other electrical characteristics.

The rotor resistance determines the slope of the torque (power) vs rotor speed curve. The torque (power) is roughly proportional to the rotor speed also when the model is non-linear as long as the power is less than 1.5-1.7 times nominal power.

For variable speed systems the generator dynamics plays an important role in the design of the speed loop controller. The parameters used to describe the generator also have an important impact on the overall system behavior. Especially important is the rotor resistance for the damping of the system, (Bindner et al, 1993).

2.4 Pitch system

The pitch system consists of an amplifier, a hydraulic piston with a position transducer and the blades. When the piston moves the three blades turn. The system work in a closed loop as a position servo. The system is non-linear due to both the mechanical system and the hydraulic system. The dynamic behavior of the pitch servo is modelled as a simple linear low order transfer function based on step responses. The order of the transfer function as well as the parameters are fitted from measured data. This is done later in the Model Estimation Chapter.

A detailed model is not considered necessary for the design of pitch controllers as the real pitch system is tuned to have first order characteristics.

2.5 Aerodynamics

The aerodynamic part of the wind turbine is split in two. The first one is the normal steady state behavior. The second part is the dynamic effect as a result of changing the pitch. This effect is known as Induction or Wake Delay. Both aerodynamic submodels are linearized models.

2.5.1 Torque and Thrust Coefficients

The power developed on the main shaft is given by eg. (Andersen 80)

$$P_{aero} = \frac{1}{2}\rho\pi R^2 u_w^3 C_p(u_w, \theta_p) \tag{12}$$

and the torque

$$T_{aero} = \frac{P_{aero}}{\omega_{rs}} \tag{13}$$

The thrust on the rotor is determined by

$$F_{aero} = \frac{1}{2}\pi R^2 u_w^2 C_T(u_w, \theta_p) \tag{14}$$

These equations are nonlinear in the wind speed, pitch angle and angular velocity of the rotor. Constant angular velocity is assumed in the following.

The torque is linearised as

$$\Delta T_{aero} = \frac{\partial T_{aero}}{\partial V}\Delta V + \frac{\partial T_{aero}}{\partial \theta}\Delta\theta \tag{15}$$

and the thust similarly.

The torque and thrust coefficients for the linearised model are found simply by finding the local derivatives of the torque and thrust surfaces of the turbine with respect to pitch angle and wind speed. The torque and thrust surfaces are calculated numerically by a separate aerodynamic program, ADYN (Adyn 85). The result of this calculation is a matrix for each of the two parameters. The contour plot of the shaft torque is shown on figure 4.

It is seen that for certain pitch angles/wind speeds the derivatives are zero. Also the derivatives change sign. In figure 4 the torque and thrust coefficients are shown at three different torque levels.

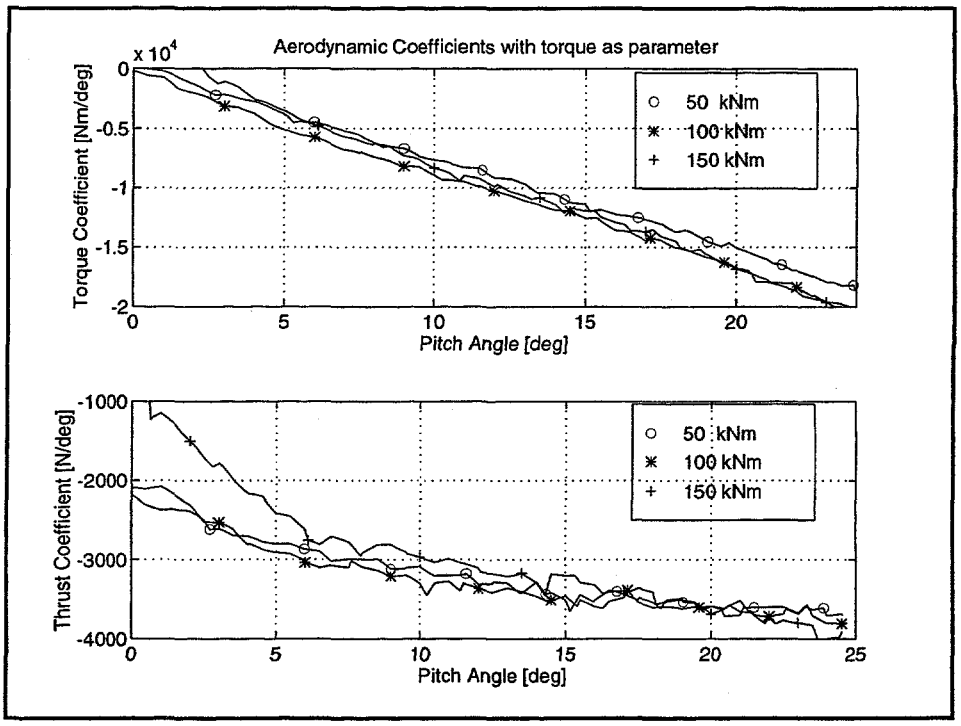

figure 5 Aerodynamic coefficients: Above: Torque, below: Thrust

The torque coefficient is almost proportional to the pitch angle at all the three levels. The thrust coefficient also changes with the pitch angle. The change in torque

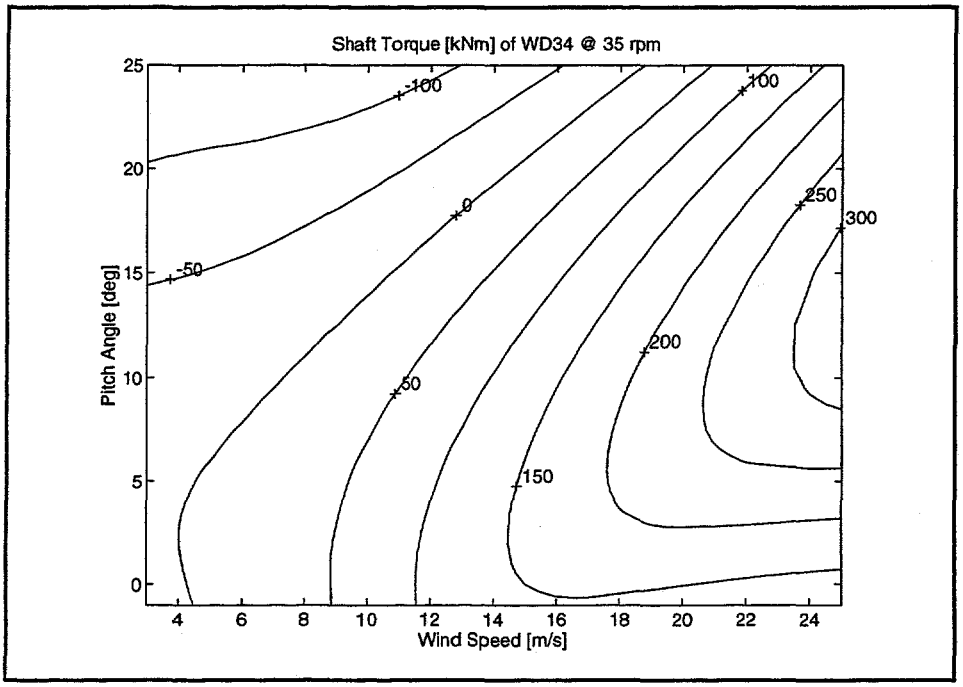

figure 4 Contour plot of shaft torque (WD34 @ 35 rpm)

coefficient has to be compensated for in the pitch controller to have almost the same loop gain in all the operating points. This can be done either by gain scheduling or by adaptive control.

2.5.2 Induction Delay

An important effect when applying pitch control is the induction delay or wake delay, (Øye 86), (Snel 92), which is a delay in the changes of induction produced by the wind turbine. This effect is seen when the pitch angle is changed quickly. It then takes some time to reach the new steady state and initially it looks as if the change of pitch angle has been larger than it actually is. The effect is modelled as a lead-lag filter with zero DC-gain in parallel with a constant gain (the torque and thrust coefficients), figure 6.

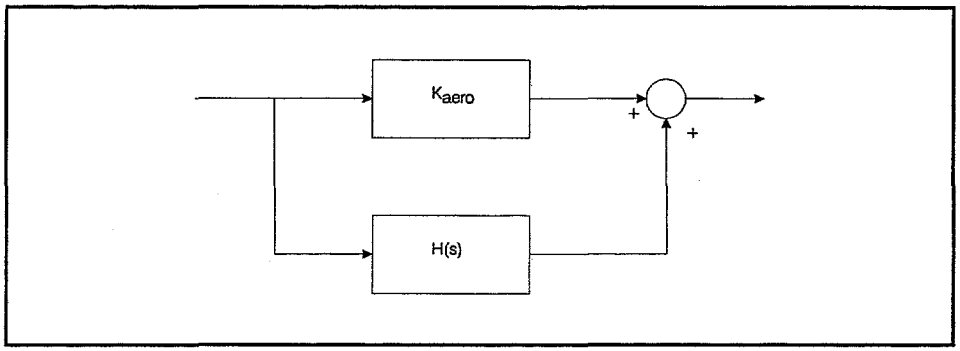

figure 6 Modelling of Induction Lag. K_{aero} is the aerodynamic coefficient and H(s) is a lead-lag filter with zero dc gain.

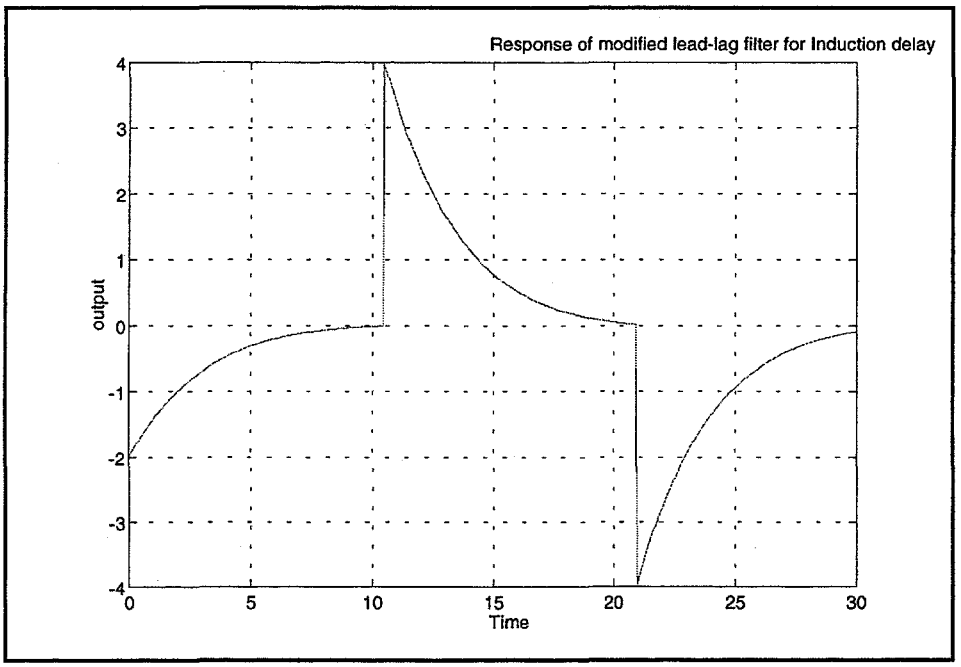

figure 7 Step response of Induction delay part

The induction lag is implemented as in (16) (in Laplace domain). The gain at DC is zero so the induction lag part is only visible when the pitch changes. The time response

of the dynamic part on a step is shown in figure 7. Since the induction lag exists independently of the static gain it is implemented in parallel with this. It is then possible to model the effect also at wind speeds where the aerodynamic coefficients are zero (or very small, see below).

$$Y(s)=\frac{gain\cdot k\cdot s(s+\frac{1}{\tau_1 k})}{(s+\frac{1}{\tau_2})(s+\frac{1}{\tau_1})}U(s) \;=\; H(s)\;U(s) \tag{16}$$

The values of the constants in the model are found from measurements, see below. The time constants and k can be chosen to be the same for the thrust and the torque. The gain is very different for the two signals, thrust and torque.

2.6 Sensors

The sensors may have an important impact on the overall behaviour of a control system. To takes this into account the sensor of the system is modelled. This is the power transducer. The sensor model is simple. It includes a time constant and a gain.

$$y_m=\frac{k_{sensor}}{\tau_{sensor}s+1}y \tag{17}$$

The parameters are found from the datasheets.

2.7 Controllers

The controllers implemented in the model are linear digital controllers. The compensation for the non-linear behaviour of the aerodynamics will be implemented in the controller in the real system. Likewise, the proportional gain in the controller model is adjusted to the operating point . Limitations on the control signal will be ignored in the model. The input to the controller is the measured power (and the power reference) and the output is the pitch angle. This is the input to the pitch servo system.

For validation purposes and for comparisons the time discrete PI-controller of the real turbine is implemented in the model. The parameters of the controller in the model is the same as on the real turbine and the proportional gain is adjusted according to the operating point.

3 Model Parameter Estimation

To find different model parameter values some specific measurements have been carried out. These measurements are used both to check the model structure and to find suitable parameter values, when there is no theoretical way to calculate them.

3.1 Shaft stiffness and damping

To find the parameter values for the torsional stiffness of the main shaft a braking sequence was performed. The rotor was accelerated and when a certain speed was

reached it was braked. The rotor then oscillates. The frequency of the oscillation is determined by the inertia of the rotor and the stiffness of the main shaft

$$\omega = \sqrt{\frac{K_{shaft}}{I_{rotor}}} \tag{18}$$

This frequency is found from the time trace in figure 8 which shows the torque on the main shaft.

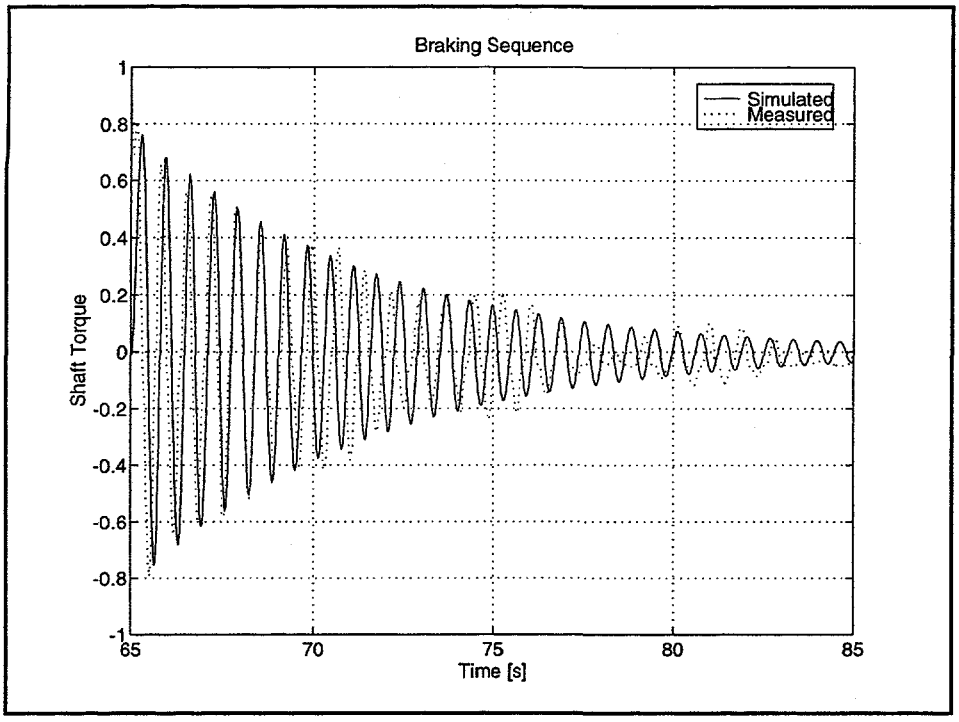

figure 8 Braking Sequence. Full line: simulated. Dotted line : measured.

The response of the simulation model is fitted to this frequency by adjusting the stiffness of the main shaft.

The simulated response is also shown in figure 8. A slight difficulty when comparing the simulated response with the measured is that the measured response includes slack.

3.2 Induction delay

The importance of including a model of induction delay is clearly seen in figure 9. The figure shows the response of the power on a step in pitch angle. The measured time series contains more than 20 periods with square wave excitation. To make the lag more visible the data is averaged over 20 periods of a square wave signal. The average output from the turbine during the measurement period was 40 kW. The results shown in figure 9 and figure 10 are deviations from the average values of the time series.

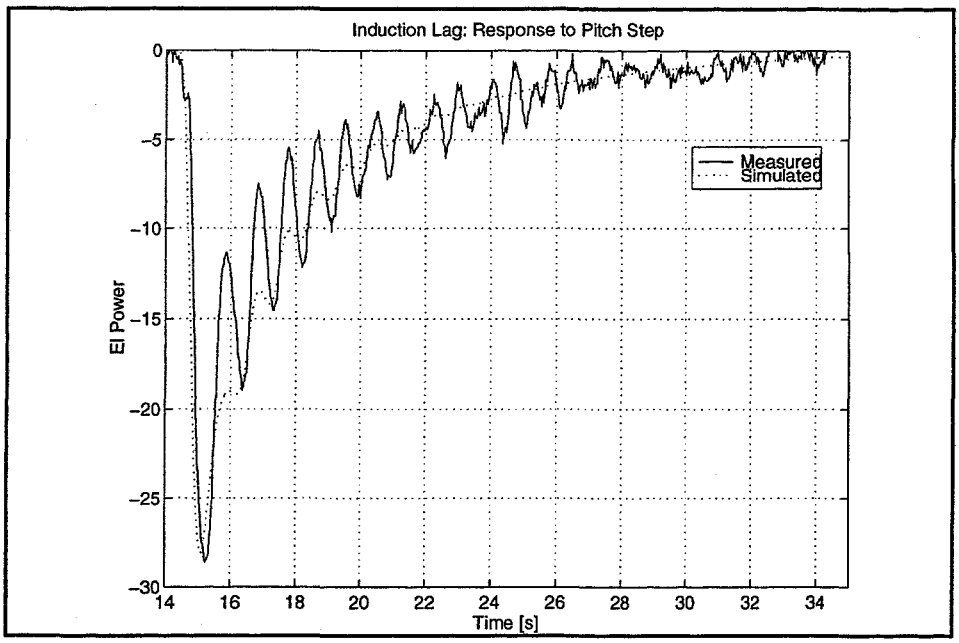

figure 9 Induction lag: Response on pitch step. Electrical power. Full line: simulated. Dotted line: measured. Average wind speed= 6 m/s, pitch angle =0.5-2.5 deg, average power = 40 kW.

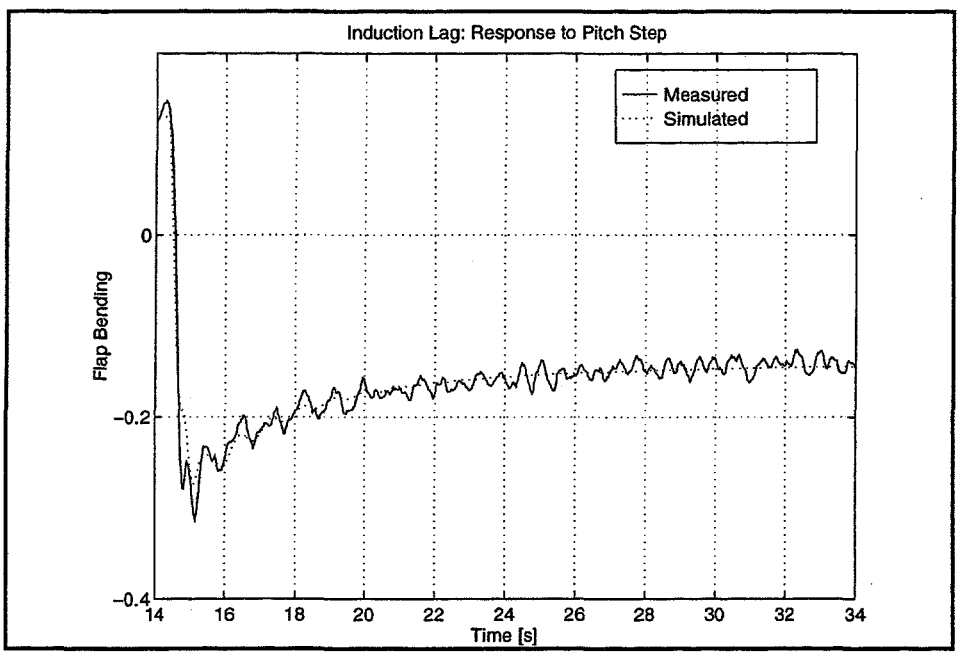

figure 10 Induction lag: Response on pitch step. Flap bending. Full line: simulated. Dotted line: measured. Average wind speed = 6 m/s, pitch angle = -0.5-2.5, average power = 40 kW.

The response of the power on a pitch step is shown in figure 9. The response shows very clearly the dynamics of the induction delay. The measurement was carried out at low wind speeds and it is noticed that the steady state power level is the same before and after the step change in pitch angle. If the induction delay was not modelled there would only have been dynamic response without a dc offset at the time of the steps. This is caused by the change in thrust. The tower eigenfrequency is clearly visible in

the power signal.

The blade bending moment is shown in figure 10. It is seen that the blade bending moment behaves differently from the power when the pitch is changed. One reason for this is that the lift forces in absolute terms change when the pitch angle is changed. This is not true for the power at low wind speeds.

Model parameters can be fitted to the results. The time constants determines the decay of the induction lag and the gain determines the peak values. The time constants are chosen to be the same for both the thrust and the torque. The gains in the induction lag part are fitted to the measurements. The static gain is derived from the steady state aerodynamics.

By changing the model parameters it can be seen that the shape of the response depends on the eigenfrequency of the drive train. The first three periods looks very different depending on whether the eigenfrequency of the drive train is below or above the tower eigenfrequency. Shown in figure 9 is a situation where the drive train frequency is .99 Hz and the tower frequency is 1.1 Hz as is the case for WD34. The model shows that if the tower eigenfrequency is lower than the drive train the initial peak would be more pronounced and the next two peaks would outphase.

3.3 Pitch System

The transfer function of the pitch system from the reference pitch angle to the actual pitch angle is found from measurements. In figure 11 the measured response of the pitch systems on a step change of the pitch reference is shown. It is seen that the response is like a first order system. Also in the figure is the simulated response of a first order system with a time constant of 0.3s and a unit gain. The simulation fits the measured system well.

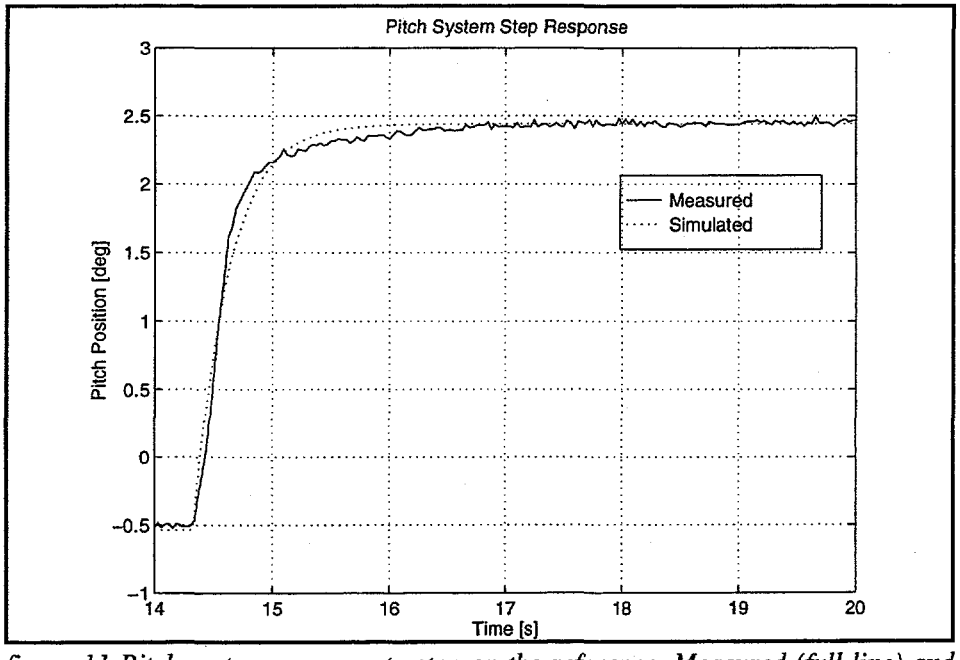

figure 11 Pitch system response to step on the reference. Measured (full line) and Simulated (dotted)

4 Validation of the total model

4.1 Open Loop validation

The open loop operation of the turbine is when the power limitation loop is opened. The pitch servo loop is closed at all times. Validating the model when it is operating in open loop mode, data from step responses on the pitch reference are used as well as sequences where the pitch reference is excited by a random signal. It is relatively simple to carry out simulations with the model. Another advantage of imploying step changes is that by doing that several times during one run it is possible to average out the wind disturbance and isolate the effect of pitch changes.

The transfer function from pitch angle to electrical power has been measured. It was done in two ways. The transfer function has been estimated from a fft of time signals when the pitch system has been excited by a square wave and by a random signal. The estimates is valid up to approx. 1.2 Hz, figure 12 (square wave), and 3 Hz, figure 13 (random noise).The difference in frequency range is due to the energy at the higher frequencies is higher in the random signal. At higher frequencies the coherence between input and output is almost zero. The measured transfer function is plotted in figure 12 and figure 13, both the amplitude and the phase. The simulated transfer function is also on the plots.

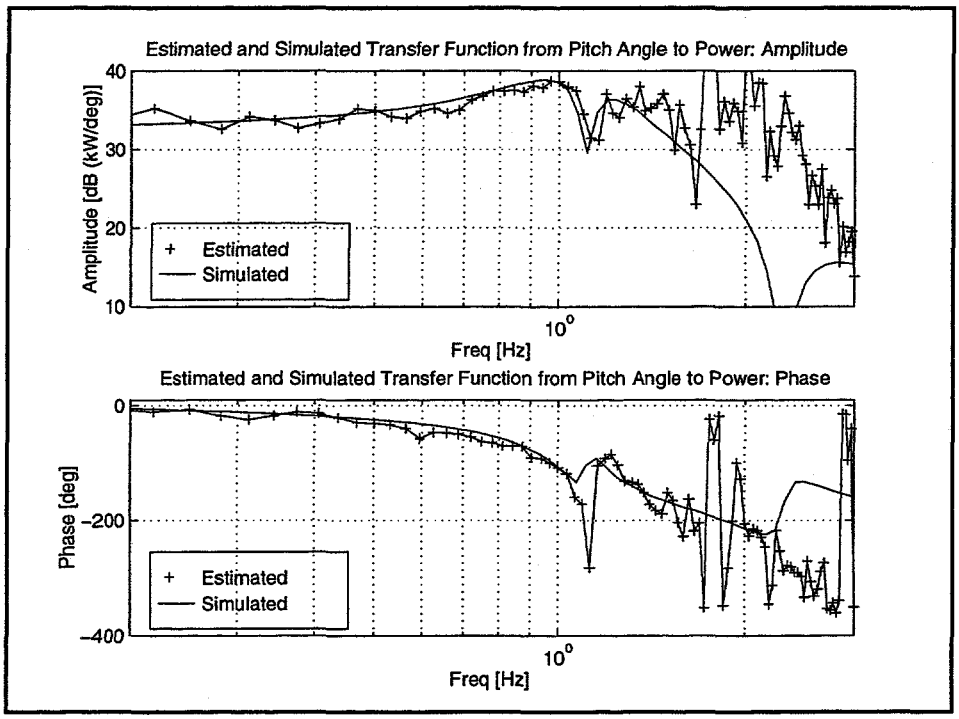

figure 12 Transfer function from pitch angle to electrical power (square wave excitation). Measured (+) and Simulated. Average wind speed = 14.4 m/s, pitch angle = 10-12 deg, average power = 345 kW.

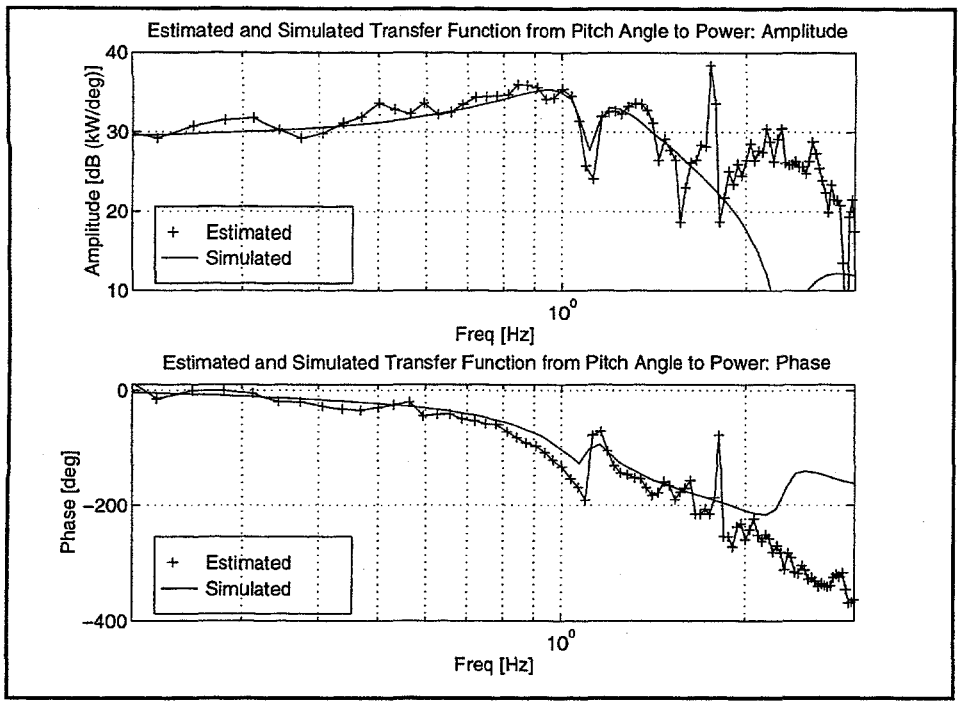

figure 13 Estimated and simulated open loop transfer function from pitch angle to power (random signal excitation). (+ Estimated, - Simulated). Average wind speed = 9.5 m/s, average pitch angle = 7.1 deg, average power = 133 kW.

It is seen that the shape of the simulated transfer function compares well with the measured. The amplitude has the correct level and the 'dip' at the tower eigenfrequency (1.1 Hz) is predicted correctly. The estimated phase in figure 13 @ 9.5 m/s consistently lies below the simulated. The phase of the simulated transfer function in figure 12 @ 14.4 m/s fits the estimated much better. It should be noticed that the amplitude of the transfer function changes with the mean wind speed as was described in the chapter on aerodynamic parameters . Note that the model predicts these changes in amplitude.

At frequencies in the range 1.7-3 Hz there is a peak in amplitude and phase like the one at 1.1 Hz caused by the tower oscillations. The model predicts a similar peak at 2.3 Hz due to the symmetric flap bending. The peak in the estimated transfer function is not explained by the model since the other mesurements indicate that the symmetric flap bending is placed at 2.3 Hz. The peak might be caused by torsional bending of the blades, but this has not been investigated.

4.2 Closed Loop Validation

The model has also been validated when the power control loop is closed. A linear model of the PI-controller on the real turbine has been implemented, and the controller parameters as well as the aerodynamic parameters have been calculated at the operating point of the turbine when the measurement was carried out.

During the measurement the turbine was exited by a square wave signal on the power reference input to the PI-controller (400 kW ± 40 kW, 40 s). After that the transfer function from power reference to power output was estimated by calculating the fft of input and output signals as it was done when the system was operating in open loop. As for the open loop the estimate is valid up to approx. 1.2 Hz.

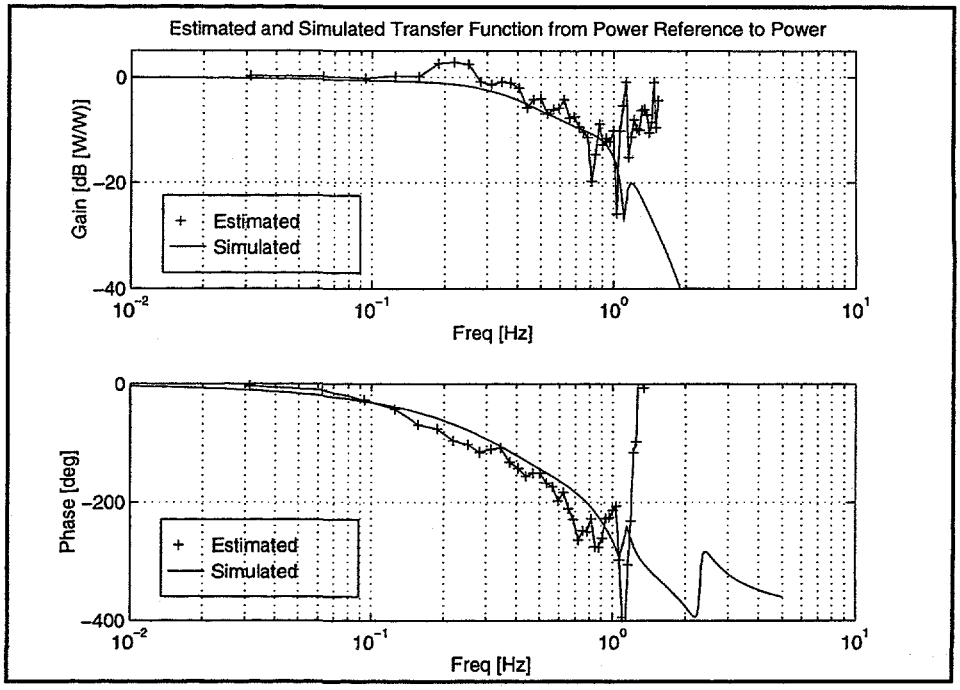

figure 14 Transfer function from power reference to electrical power. Estimated (+) and simulated. average wind speed = 15 m/s, average pitch angle = 10.1 deg , average power = 412 kW.

The estimated and simulated transfer function are plotted in figure 14. It is noticed the correspondence is good up to 1 Hz. Above that the estimate is not well determined.

5 Model Discussion

The developed model describes in adequate details the behavior of a turbine with respect to designing and analyzing pitch controllers. In the present context the transfer functions of interest is the transfer function from pitch angle to electrical power and from free wind speed to electrical power. The frequency range of interest is 0-3 Hz.

The transfer function from pitch angle to electrical power in this frequency range is mainly determined by the drive train and the first tower bending mode. The symmetrical flap bending mode is also of some importance.

The eigenfrequency of the drive train is relatively undamped with a relative damping of ca. 0.25. The tower bending influences the transfer function with both a pole pair and a zero pair of the same length. This results in the phase shift at 1.1 Hz. At higher frequencies the flap mode is visible (2.3 Hz) in the same way as the tower mode. The measurements indicates that there should be a peak at ca. 1.8 Hz.

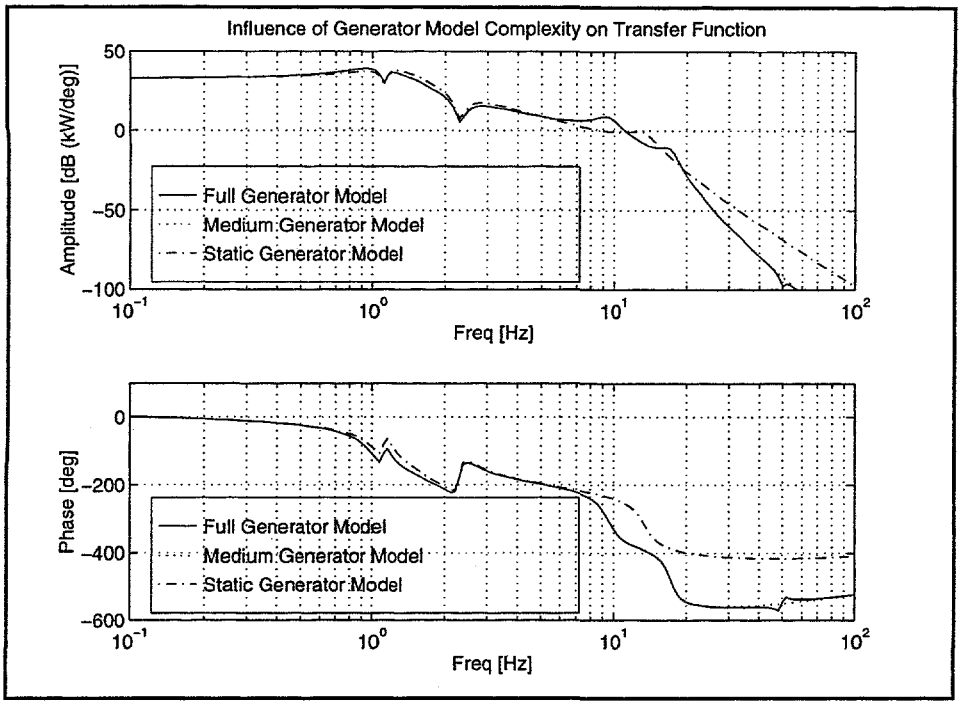

figure 15 The transfer function dependence on generator dynamics.

The generator dynamics are fast compared with the drive train and structural dynamics. This is illustrated in figure 15, which shows that the full dynamic model and the medium dynamic model differs only slightly even at high frequencies. The static model changes the damping of the system but the behavior is similar to the two other models. The medium complex model is used as nominal model.

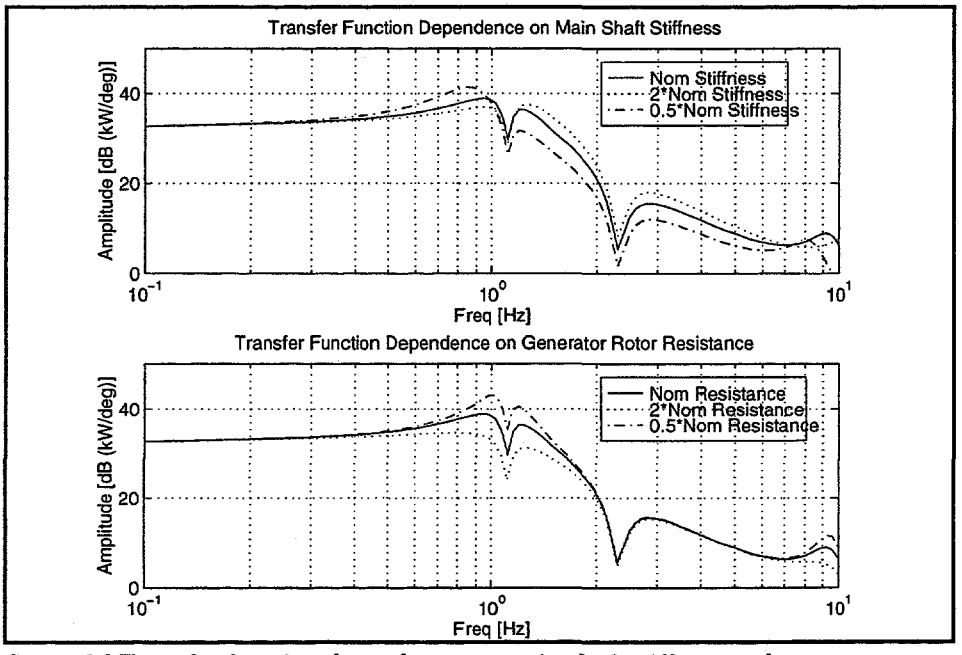

figure 16 Transfer function dependence on main shaft stiffness and generator rotor resistance.

In (Bindner 93) the influence of the stiffness of the main shaft and the slip of the

generator on the transfer function is shown. In figure 16 it is seen how the stiffness of the shaft and the slip (rotor resistance) changes the transfer function in the region around the eigenfrequency of the drive train. Especially a higher slip improves the shape of the transfer function and makes it easier to obtain a sufficient closed loop bandwidth.

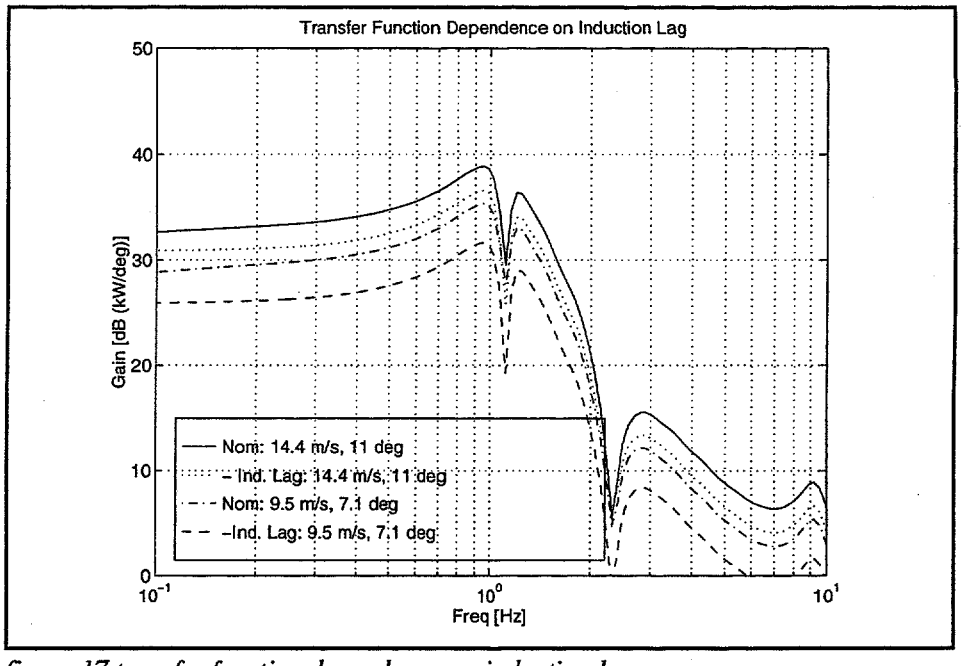

figure 17 transfer function dependence on induction lag.

In figure 17 is shown how the induction lag changes the gain of the transfer function from pitch angle to power. In two different operating points the gain is plotted with and without the induction lag included in the model. It is clearly seen how the induction lag increases the gain with 2.5 dB resp. 3.6 dB at high resp. low wind speeds. The figure also illustrates how the gain changes with wind speed and pitch angle. The gain is increased with wind speed and pitch and in the wind speed and pitch angle ranges shown.

6 Conclusion

This report presents a linearised wind turbine model which includes dynamic models of the tower and rotor, the drive train and the aerodynamics. The presented model describes in adequate details the behavior of a turbine with respect to design and analysis of pitch controllers. The model is relatively simple and only the necessary dynamics have been included. It has been validated against measurements and up to 1.2 Hz there is a fine correspondance between the measured and the simulated behavior when the transfer function from pitch angle to electrical power is considered. To describe the system adequately the model needs to include the first tower bending mode but the generator can be modelled simply as a damper.

The model is well suited for controller design because of the low number of states. For detailed analyses of the behavior of a pitch controlled turbine a more comprehensive model with an enhanced description of especially the aerodynamics is necessary.

References

Andersen, P.S., U. Krabbe, P. Lundsager, H. Petersen. Basis Material for Wind Turbine Design. Risø-M-2153, January 1980 (in Danish).

ADYN 1985. Aerodynamic performance code.

Bindner, H., P.H. Madsen, K.E.Thomsen, K. Andersen (1993). Active Pitch Control: The Controllers Influence on Performance and Loads of a Wind Turbine. In: Proceedings of ECWEC'93, Travemünde, Germany, March 1993

Bindner, H. (1999) The relation between main shaft torque and electrical power, Risø-I-1436[DA], Juli 1999 (in Danish).

Bongers, P, T. van Engelen, S. Dijkstra, Z-J. Kock (1989). Optimal Control of a Wind Turbine in Full Load - a case study. In: Proc of EWEC'89, Glasgow, UK, 10-13 July 1989.

Bongers, P.M.M, G.E. van Baars, S. Dijkstra (1993a). Load Reduction in a Wind Energy Conversion System Using a H∞ Controller. In: Proc. of IEEE 2nd Conference on Control Application.

Bongers, P.M.M, G.E. van Baars, S. Dijkstra (1993b). DUWECS: A Wind Turbine Design Tool. In: Proc. of Windpower'93.

Bossanyi, E.A. (1989). Adaptive Control of the MS2 Wind Turbine - Practical Results. *Wind Engineering Vol13 No. 5*

Grimble, M.J., S.A. De La Salle, D. Reardon, W.E. Leithead (1990). A Lay Guide to Control Systems and their Application to Wind Turbines. In: Proceeding of BWEA'90, UK.

Jørgensen, H.K. (1993). Adaptive Pitch Control of Wind Turbines. M Sc. dissertation from IMSOR, DTU Lyngby Denmark.

Klingenberg, B. (1991). Adaptive Pitch Control for Wind Turbines. M Sc. dissertation from IMSOR, DTU Lyngby Denmark.

Kovacs, P.K.: Transient Phenomena in Electrical Machines. Elsevier, Amsterdam 1984.

Knudsen, T. (1983). Control of Wind Turbines. M Sc. dissertation from IMSOR, DTU Lyngby Denmark (in danish).

Leithead, W.E., S.A. De La Salle, D. Reardon (1990). Classical Control of a Pitch Control System. In: Proceeding of BWEA'90, UK.

Madsen, P.H., Sfrandsen (1989). Pitch Angle Control for Power Limitation. In: Proceedings of EWEC'89, Glasgow, UK, 10-13 July 1989.

Matlab Reference Guide (1994) MathWorks, MA, USA.

Mattson, S.E. (1985). Modelling and Control of a Large Horizontal Axis Wind Power Plant. Ph D. thesis, Lund University, Sweden, 1985.

Snel H., J.G. Schepers, (1992). Joint Investigation of Dynamic Inflow Effects and Implementation of an engineering Method for response Calculations. In: Proceedings of Contractor Meeting Alghero, Italy, June 1992

WEG (1989). Adaptive Pitch Control for Power Regulation of the MS-2 Wind Turbine. Contractor Report ETSU WN 5098.

Wilkie, J., W.E. Leithead, C. Anderson (1990). Modelling of Wind Turbines by Simple Models. *Wind Engineering Vol. 14 No. 4.*

Xin, M. (1993). Modelling and Control of a Wind Turbine. M Sc. dissertation from IMSOR, DTU Lyngby Denmark.

Øye, S. (1986). Unsteady Wake effects Caused By Pitch-angle Changes. In: IEA Joint action on Aerodynamics, Oct 1986.

Appendix A: List of Symbols

Structural model

M	Mass matrix
M_n	Mass of nacelle
$\tilde{m}_i$	Equivalent mass of tower
$\tilde{m}$	Equivalent mass of blade (depending on which eom see app A)
C	Damping matrix
K	Stiffness matrix
K_t	Equivalent stiffness of tower
K_b	Equivalent stiffness of blades (flapwise)
K_s	Torsional stiffness of main shaft
Q	Generalised loads matrix
Q_1	The wind and pitch angle dependent part of the linearised generalised loads
Q_2	The part of the linearised generalised loads that depends on the time derivative of the states
Q_0	The average of the generalised loads at the operation point
x	State vector
u_t	Nacelle position
u_b	Tip position
θ_{rs}	angular position of main shaft at rotor end
θ_{gs}	angular position of main shaft at gear box end
Δu_w	wind speed at rotor (deviation from operation point)
$\Delta\theta_p$	pitch angle (deviation from operation point)

Gear box

I_{gs}, I_{gf}	inertia of gear on slow resp. fast side of the gear
I_{gen}	inertia of the generator rotor
f	gear ratio
K_{fs}	stiffness of the fast shaft
C_{fs}	damping of the fast shaft
T_{ms}	torque of the main shaft, input
T_{ag}	air gap (reaction) torque of the generator, input
ω_{gs}	angular velocity of the slow shaft on the gear box, output
ω_{gen}	angular velocity of generator rotor, output

Induction generator

u_s	stator voltage
ψ_s	stator flux
ψ_r	rotor flux
ω	grid frequency
ω_r	generator rotor speed
p_{el}	electrical power
T_{ag}	reaction torque (airgap)
R_s	stator resistance
R_r	rotor resistance
L_s	stator inductance
L_r	rotor inductance
L_M	mutual inductance
σ	leakage factor

Induction lag

gain
k
τ_1
τ_2

Sensor

k_{sensor}
τ_{sensor}

Appendix B: Wind Turbine Dynamics

B.1 Simplified Structual Model of a Wind Turbine

A simplified model of a wind turbine is derived. It will be used to model the dynamic behaviour of the structure of the wind turbine.

The following degrees of freedom are included:

- The fundamental tower bending mode. It is assumed that the nacelle is not rotated when the tower is bending.
- The fundamental flap bending mode. It is assumed that the flap bending is perpendicular to the rotor plane.
- The fundamental rotor mode in the rotor plane. It is assumed it can be modelled as torsion in the main shaft.

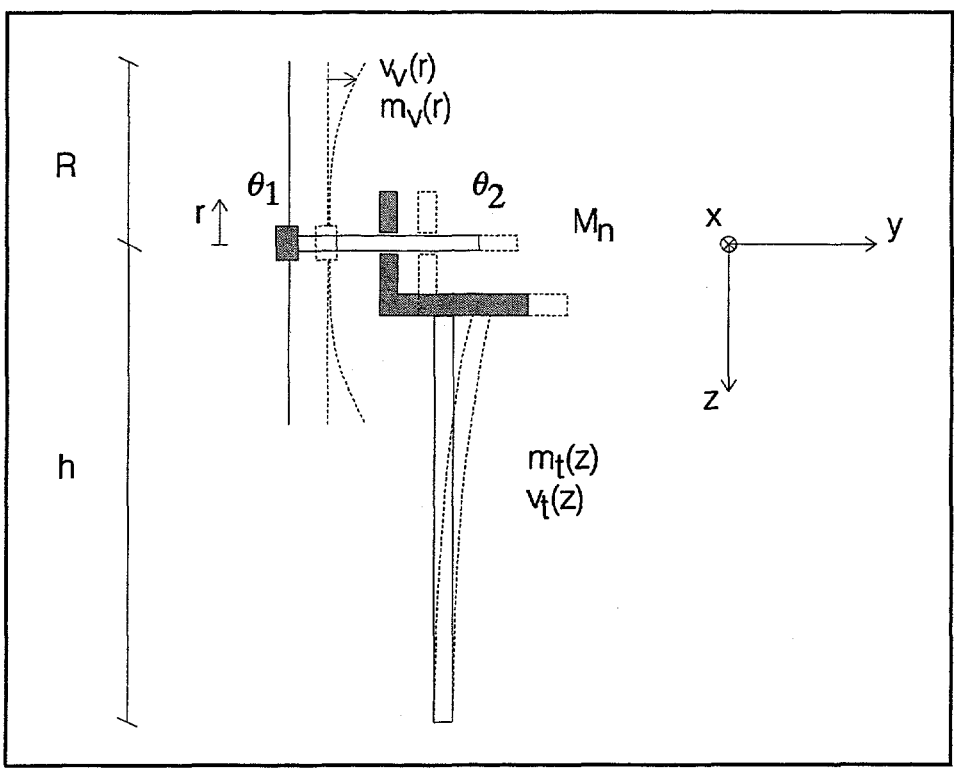

figure 18 Structural model

Bendings perpendicular to the rotor plane

Tower:

$$v_t(z)=v_0\varphi_t(z) \quad ; \quad \varphi_t(0)=1.0 \tag{1}$$

Tower Top:

$$v_t(0)=v_0 \tag{2}$$

Nacelle:

$$v_0 \tag{3}$$

Blades:

$$v_v(r)=v_0+v_b\varphi_v(r) \quad ; \quad \varphi_v(R)=1.0 \tag{4}$$

Bendings in the rotor plane

Blades

$$u_v^m(r)=\theta_1 r \tag{5}$$

Free end of main shaft

$$\theta_2 \tag{6}$$

Lagrange's equations:

Lagrange equation is used to find the equations of motion

$$\frac{\partial}{\partial t}\left(\frac{\partial T}{\partial \dot{q}_i}\right)-\frac{\partial T}{\partial q_i}+\frac{\partial V}{\partial q_i}=Q_i \tag{7}$$

where

T total kinetic energy
V total potential energy
q_i generalised coordinates
Q_i generalised load corresponding to q_i

The kinetic energy

The kinetic energy of the system is first found. The kinetic energy is the sum of the contributions from each part of the system, tower, nacelle and blades.

$$T=\frac{1}{2}M_n\dot{v}_0^2+\frac{1}{2}\tilde{m}_t\dot{v}_0^2+\frac{1}{2}3\left[\tilde{m}_v^1\dot{v}_0^2+\tilde{m}_v^2\dot{v}_0\dot{v}_b+\tilde{m}_v^3\dot{v}_b{}^2\right]+\frac{1}{2}3\tilde{m}_v^4\dot{\theta}_1{}^2 \qquad (8)$$

where

$$\tilde{m}_t=\int_0^h m_t(z)\varphi_t(z)dz \qquad (9)$$

$$\tilde{m}_v^1=\int_0^R m_v(r)dr \qquad (10)$$

$$\tilde{m}_v^2=\int_0^R m_v(r)\varphi_v(r)dr \qquad (11)$$

$$\tilde{m}_v^3=\int_0^R m_v(r)\varphi_v(r)^2dr \qquad (12)$$

$$\tilde{m}_v^4=\int_0^R m_v(r)r^2dr \qquad (13)$$

The potential energy

The systems potential is the sum of the contributions of the each of the stiffnesses, tower, blade and main shaft.

$$V=\frac{1}{2}K_t u_0^2+\frac{1}{2}3K_v v_b^2+\frac{1}{2}K_h(\theta_1-\theta_2)^2 \qquad (14)$$

where

$$K_t=\int_0^h EI_t(z)\varphi_t''(z)^2dz \qquad (15)$$

$$K_v = \int_0^R EI_v(z)\varphi_v''(r)^2 dr \tag{16}$$

$$K_h = \frac{Gk}{l} \tag{17}$$

Generalised coordinates

The generalised coordinates of the system are chosen as

- v_0 tower top position
- v_b blade tip position
- θ_1 rotor angular position
- θ_2 main shaft free end angular position

Using the equations for potential and kinetic energy the following two equations can be derived

$$\frac{\partial V}{\partial q_i} = \begin{bmatrix} K_t & & & \\ & 3K_v & & \\ & & K_h & -K_h \\ & & -K_h & K_h \end{bmatrix} \begin{bmatrix} v_0 \\ v_b \\ \theta_1 \\ \theta_2 \end{bmatrix} \tag{18}$$

$$\frac{\partial}{\partial t}\left(\frac{\partial T}{\partial \dot{q}_i}\right) = \begin{bmatrix} M+\tilde{m}_t+3\tilde{m}_v^1 & 3\tilde{m}_v^2 & & \\ 3\tilde{m}_v^2 & 3\tilde{m}_v^3 & & \\ & & 3\tilde{m}_v^3 & \\ & & & 0 \end{bmatrix} \begin{bmatrix} \ddot{v}_0 \\ \ddot{v}_b \\ \ddot{\theta}_1 \\ \ddot{\theta}_2 \end{bmatrix} \tag{19}$$

B.2 Generalised loads

The only load that will be considered is the load on the blades caused by the wind in a operating point charicterised by

- u_0 mean wind speed
- θ pitch angle
- ω rotational speed

It will also be assumed that the wind load can be factorised as

$$p(x,z,t)=q(t)\eta(r) \quad \wedge \quad r=\sqrt{(x^2+z^2)} \tag{20}$$

where $\eta(r)$ is the blade load distribution

Perpendicular to the rotor plane

Assume that the blade loads can be linerised as

$$p^1(x,z,t)=\eta(r)[q_1^0+\mu_1 v(t)] \tag{21}$$

at a wind speed $u = u_0 + v$
The thrust on rotor then is

$$F=3q_1^0\int_0^R \eta(r)dr \tag{22}$$

without fluctuation in the wind speed (v=0). With the thrust decribed by

$$F(u_0+v,\theta_0+\Delta\theta,\omega)=F(u_0,\theta_0,\omega)+\frac{\partial F}{\partial u_0}v+\frac{\partial F}{\partial \theta_0}\Delta\theta \tag{23}$$

The following can be found

$$\frac{\partial F}{\partial u_0}=3\mu_1\int_0^R \eta(r)dr \tag{24}$$

$$\frac{\partial F}{\partial \theta_0}=3\mu_5\int_0^R \eta(r)dr \tag{25}$$

In the rotor plane

Assume that the blade loads can be linearised as using

$(u=u_0+v \ , \ \omega=\omega_0+\Delta\omega \ , \ \theta=\theta_0+\Delta\theta)$

$$p^2(x,z,t)=\eta(r)[q_2^0+\mu_2 v+\mu_3\Delta\omega+\mu_4\Delta\theta] \tag{27}$$

The rotor torque can be written as

$$M(u_0+v,\theta_0+\Delta\theta,\omega_0+\Delta\omega)=M(u_0,\theta_0,\omega_0)+\frac{\partial M}{\partial u_0}v+\frac{\partial M}{\partial \omega_0}\Delta\omega+\frac{\partial M}{\partial \theta_0}\Delta\theta \tag{28}$$

where

$$\frac{\partial M}{\partial u_0}=3\mu_2\int_0^R r\eta(r)dr \tag{29}$$

$$\frac{\partial M}{\partial \omega_0}=3\mu_3\int_0^R r\eta(r)dr \tag{30}$$

$$\frac{\partial M}{\partial \theta_0}=3\mu_4\int_0^R r\eta(r)dr \tag{31}$$

If F and M known are as functions of u, θ, ω the aerodynamic influens factors μ_i can be calculated from the equations above.

The resulting generalised loads are then

$$Q=\begin{bmatrix} F+\sum_{i=1}^{3}\int_0^R \eta(r)[\mu_1(u(x_i,z_i,t)-u_o-\dot{v}_0-\dot{v}_b\varphi_v(r))+\mu_5\Delta\theta]dr \\ \sum_{i=1}^{3}\int_0^R \eta(r)[q_1^0+\mu_1(u(x_i,z_i,t)-u_o-\dot{v}_0-v_b\varphi_v(r))+\mu_5\Delta\theta]\varphi_v(r)dr \\ \sum_{i=1}^{3}\int_0^R \eta(r)[q_2^0+\mu_2(u(x_i,z_i,t)-u_o-\dot{v}_0-v_b\varphi_v(r))+\mu_3(\dot{\theta}_1-\omega_0)+\mu_4\Delta\theta]rdr \end{bmatrix} \tag{32}$$

Is it further assumed that the structural damping can be described by

$$\sigma=E\varepsilon(t)+c_s\dot{\varepsilon}(t) \tag{33}$$

the system of equations can be formulated as

$$M\ddot{x}+C\dot{x}+Kx=Q \tag{34}$$

where

M is given by (19)
K is given by (18),

$$C=\frac{c_s}{E}K \quad \text{and}$$

$$x=\begin{bmatrix} u_0 \\ v \\ \theta_1 \\ \theta_2 \end{bmatrix}$$

Notice that Q is linear in $\dot{u}_0$, $\dot{v}$, $\dot{\theta}_1$. If this part of the load is moved to the left hand side of (34) it will act as aerodynamic damping.

To make the model operational it is rearranged into a state space model. The free end of the main shaft is pulled out as an input and the load is splitted in three parts: the aerodynamic damping part, the input part and level at the linearisation point.

The original equation

$$M\ddot{x}'+C\dot{x}'+Kx'=Q_0+Q_{ac}+Q_{in}\begin{bmatrix} v \\ \Delta\theta \end{bmatrix} \tag{34}$$

is rearranged to a the state space model

$$\begin{aligned} \dot{x}&=Ax+Bu \\ y&=Cx+Du \end{aligned} \tag{35}$$

The new state vector is

$$x=\begin{bmatrix} u_0 \\ v \\ \theta_1-\theta_2 \\ \dot{u}_0 \\ \dot{v} \\ \dot{\theta}_1 \end{bmatrix} \tag{36}$$

and the input and output vectors

$$u=\begin{bmatrix} F_t \\ F_v \\ M \\ \dot{\theta}_2 \end{bmatrix} \quad and \quad y=M_{shaft} \tag{37}$$

The system matrices are

$$A=\begin{bmatrix} & & 1 & \\ & \underline{\underline{0}} & & 1 \\ & & & 1 \\ -M^{-1}K & & & -M^{-1}(C-Q_{ac}) \end{bmatrix} \tag{38}$$

$$B=\begin{bmatrix} 0 & 0 & 0 & 0 \\ 0 & 0 & 0 & 0 \\ 0 & 0 & 0 & -1 \\ -M^{-1}[I & & \begin{bmatrix}0\\0\\C_h\end{bmatrix} &] \end{bmatrix} \tag{39}$$

and

$$C=[0 \;\; 0 \;\; K_h \;\; 0 \;\; 0 \;\; C_h] \text{ and } D=[0 \;\; 0 \;\; 0 \;\; -K_h \tag{40}$$

where

$$M=\begin{bmatrix} M+\tilde{m}_t+3\tilde{m}_v^1 & 3\tilde{m}_v^2 & 0 \\ 3\tilde{m}_v^2 & 3\tilde{m}_v^3 & 0 \\ 0 & 0 & 3\tilde{m}_v^4 \end{bmatrix} \tag{41}$$

$$K=\begin{bmatrix} K_t & 0 & 0 \\ 0 & 3K_v & 0 \\ 0 & 0 & K_h \end{bmatrix} \tag{42}$$

$$C=\begin{bmatrix} C_t & 0 & 0 \\ 0 & 3C_v & 0 \\ 0 & 0 & C_h \end{bmatrix}=const*K \tag{43}$$

The aerodynamic matrices are given by

$$Q_{ac}=\begin{bmatrix} -k_1 & -k_2 & 0 \\ -k_2 & -k_7 & 0 \\ -k_3 & -k_8 & k_9 \end{bmatrix} \text{ and } Q_{in}=\begin{bmatrix} k_1 & k_2 \\ k_3 & k_4 \\ k_5 & k_6 \end{bmatrix} \tag{44}$$

where the k-constants are defined by

$$k_1=\frac{\partial F}{\partial u_0}, \quad k_2=k_1*\frac{\int_0^R \eta(r)\varphi(r)dr}{\int_0^R \eta(r)dr} \tag{45}$$

$$k_3=\frac{\partial M}{\partial u_0} \tag{46}$$

$$k_4=\frac{\partial F}{\partial \theta_0}, \quad k_5=k_4*\frac{\int_0^R \eta(r)\varphi(r)dr}{\int_0^R \eta(r)dr} \tag{47}$$

$$k_6=\frac{\partial M}{\partial \theta_0} \tag{48}$$

$$k_7 = k_1 * \frac{\int_0^R \eta(r)\varphi^2(r)dr}{\int_0^R \eta(r)dr} \tag{49}$$

$$k_8 = k_1 * \frac{\int_0^R \eta(r)\varphi(r)rdr}{\int_0^R \eta(r)dr} \tag{50}$$

$$k_9 = \frac{\partial M}{\partial \omega_0} \tag{51}$$

Bibliographic Data Sheet **Risø-R-920(EN)**

Title and authors

Active Control: Wind Turbine Model

Henrik Bindner

ISBN	ISSN
87-550-2216-2	0106-2840

Department or group	Date
Wind Energy and Atmospheric Physics Dept.	July 1999

Groups own reg. number(s)	Project/contract No(s)

Pages	Tables	Illustrations	References
37	0	18	22

Abstract (max. 2000 characters)

This report is a part of the reporting of the work done in the project 'Active Control of Wind Turbines'. This project aim is to develop a simulation model for design of control systems for turbines with pitch control and to use that model to design controllers.

This report describes the model developed for controller design and analysis. Emphasis has been put on establishment of simple models describing the dynamic behavior of the wind turbine in adequate details for controller design. This has been done with extensive use of measurements as the basis for selection of model complexity and model validation as well as parameter estimation.

The model includes a simple model of the structure of the turbine including tower and flapwise blade bending, a detailed model of the gear box and induction generator, a linearized aerodynamic model including modelling of induction lag and actuator and sensor models. The models are all formulated as linear differential equations.

The models are validated through comparisons with measurements performed on a Vestas WD 34 400 kW wind turbine.

It is shown that from a control point of view simple linear models can be used to describe the dynamic behavior of a pitch controlled wind turbine. The model and the measurements corresponds well in the relevant frequency range.

The developed model is therefore applicable for controller design.

The project participants are
Risø National Laboratory,
Vestas Wind Systems A/S
Kurt Andersen,The Technical University of Denmark

Descriptors INIS/EDB

CONTROL SYSTEMS; DESIGN; DYNAMICS; MATHEMATICAL MODELS; OPTIMIZATION; WIND TURBINES

Available on request from Information Service Department, Risø National Laboratory,
(Afdelingen for Informationsservice, Forskningscenter Risø), P.O.Box 49, DK-4000 Roskilde, Denmark.
Telephone +45 4677 4004, Telefax +45 4677 4013